X-ray Absorption Spectroscopic Studies of the Fe(II) Active Site of Catechol 2,3-Dioxygenase. Implications for the Extradiol Cleavage Mechanism†

Lijin Shu,‡ Yu-Min Chiou,‡ Allen M. Orville,§ Marcia A. Miller,§ John D. Lipscomb,*,§ and Lawrence Que, Jr.*,‡

Departments of Chemistry and Biochemistry (Medical School), University of Minnesota, Minneapolis, Minnesota 55455

Received November 10, 1994; Revised Manuscript Received March 13, 1995⊗

ABSTRACT: The extradiol-cleaving catechol 2,3-dioxygenase (2,3-CTD) isolated from *Pseudomonas putida* mt-2 and its catechol and ternary E•S•NO complexes are characterized by X-ray absorption spectroscopy (XAS). The intensities of the 1s→3d transitions in the pre-edge spectra of the uncomplexed enzyme and its substrate complex show that the Fe(II) center is five-coordinate in both complexes, in agreement with earlier magnetic circular dichroism studies [Mabrouk, P. A., Orville, A. M., Lipscomb, J. D., & Solomon, E. I. (1991) *J. Am. Chem. Soc. 113,* 4053−4061]. Analysis of the EXAFS region of uncomplexed 2,3-CTD shows five N/O ligand atoms 2.09 Å from the active site Fe(II). In the 2,3-CTD•catechol complex, one N/O atom is located at 1.93 Å and four N/O type ligands are at 2.10 Å. By comparison with [Fe^{II}-(6TLA)(DBCH)](ClO_4), the first well-characterized mononuclear Fe(II)•catechol model complex, the 1.93 Å scatterer is proposed to be the oxygen from the deprotonated hydroxyl group of the coordinated catecholate monoanion. Nitric oxide binds to the Fe(II) center in the enzyme•catechol complex without displacing the existing ligands, resulting in the formation of a six-coordinate complex, as indicated by the addition of a new N/O type scatterer at 1.74 Å. Bond valence sum (BVS) analysis of the bond lengths derived from the EXAFS fits gives values that correspond to the iron oxidation states established for these complexes, thus lending credence to the coordination environment deduced for the iron center in those complexes. The present study provides the first evidence for a monoanionic substrate binding mode in an extradiol dioxygenase, which is distinct from the dianionic binding mode proposed for intradiol dioxygenases. We speculate that this difference in binding mode may have important ramifications for the site of aromatic ring cleavage in the subsequent oxygen insertion reactions.

Dioxygenases catalyze the incorporation of both atoms of dioxygen into organic substrates and play important roles in metabolically important chemical transformations. Those that catalyze the cleavage of aromatic rings are among the best characterized (Lipscomb & Orville, 1992; Que, 1989). Mechanistically distinct members of this group containing Fe(II) or Fe(III) as an essential active site component have been studied extensively.[1] Catechol 2,3-dioxygenase (2,3-CTD)[2] (EC 1.13.1.2), isolated from many divergent soil bacteria, has served as the archetypical enzyme for mechanistic studies of Fe(II) type dioxygenases (Nozaki et al., 1968; Hori et al., 1973). It catalyzes the extradiol ring cleavage of catechol to form α-hydroxymuconic semialdehyde (Scheme 1). 2,3-CTD (140 kDa) purified from *Pseudomonas putida* mt-2 (formerly classified as *P. arvilla*) is composed of four identical subunits, each of which contains one Fe(II) atom essential for enzyme activity (Nakai et al., 1983).

Scheme 1

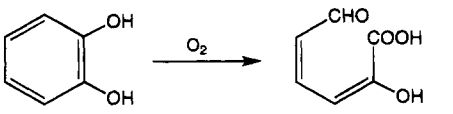

Catechol α-Hydroxymuconic semialdehyde

The lack of both optical and EPR spectra has slowed progress in understanding the coordination environments of the iron site in 2,3-CTD and its substrate complex. However, some information about the iron site has been derived from Mössbauer spectroscopy (Tatsuno et al., 1980), which showed a high-spin Fe(II) site (δ = 1.31 mm/s, ΔE_Q = 3.28 mm/s), and CD/MCD studies (Mabrouk et al., 1991), which indicated an active site with square-pyramidal geometry. Although changes in protein conformation, and even the

† This research was supported by the National Institutes of Health [GM 33162 (L.Q.) and GM 24689 (J.D.L.)]. Beamline X9 at the NSLS at BNL was supported by the NIH (RR-001633). A.M.O. and M.A.M. acknowledge traineeships from the National Institutes of Health.

* Authors to whom correspondence should be addressed.

‡ Department of Chemistry.

§ Department of Biochemistry.

⊗ Abstract published in *Advance ACS Abstracts,* May 1, 1995.

[1] The only exceptions found so far are the 3,4-dihydroxyphenylacetate 2,3-dioxygenases from *Bacillus brevis* and *Arthrobacter* strain Mn-1, which contain manganese (Que et al., 1981; Olson et al., 1992), and that from *Klebsiella pneumoniae,* which is a Mg^{2+}-containing enzyme (Gibello et al., 1994).

[2] Abbreviations: ACV, δ-(L-α-aminoadipoyl)-L-cysteinyl-D-valine; BF, benzoylformate; BVS, bond valence sum; 1,2-CTD, catechol 1,2-dioxygenase; 2,3-CTD, catechol 2,3-dioxygenase; CD, circular dichroism; DBCH, 3,5-di-*tert*-butylcatechol; EDTA, ethylenediaminetetraacetate; EXAFS, extended X-ray absorption fine structure; im, imidazole; HEPES, *N*-(2-hydroxyethyl)piperazine-*N*′-2-ethanesulfonic acid; IPNS, isopenicillin N synthase; MCD, magnetic circular dichroism; MOPS, 3-morpholinopropanesulfonic acid; PCA, 3,4-dihydroxybenzoate; 3,4-PCD, protocatechuate 3,4-dioxygenase; RMS, root mean square; 6TLA, tris[(6-methyl-2-pyridyl)methyl]amine; TMC, 1,4,8,11-tetramethyl-1,4,8,11-tetraazacyclotetradecane; TMPzA, tris[(3,5-dimethylpyrazol-1-yl)methyl]amine; TPA, tris(2-pyridylmethyl)amine; XANES, X-ray absorption near-edge spectroscopy; XAS, X-ray absorption spectroscopy.

0006-2960/95/0434-6649$09.00/0

ligand field, have been detected by CD and MCD studies (Hirata et al., 1971; Mabrouk et al., 1991), the Fe(II) center maintains its oxidation state and square-pyramidal geometry upon formation of the anaerobic substrate complex.

Similar to the studies of some other Fe(II)-containing proteins (Nelson, 1988; Rich et al., 1978; Chen et al., 1989), EPR studies of the nitrosyl adducts of 2,3-CTD (Arciero et al., 1985; Arciero & Lipscomb, 1986) have provided important information about the exogenous ligands to the Fe(II) center. The NO complex of 2,3-CTD exhibits a signal with g values near 4 and 2, typical of an $S = 3/2$ spin state. The signal is broadened by hyperfine interactions from ^{17}O-enriched water, indicative of the direct ligation of one or more solvent molecules to the iron in 2,3-CTD·NO. The EPR signals of the binary 2,3-CTD·NO complex are perturbed when substrates or inhibitors are added, demonstrating the formation of ternary E·S or E·I nitrosyl complexes. In these ternary complexes, hyperfine broadening of the EPR spectrum from ^{17}O-enriched solvent is not observed, implying solvent exclusion from the iron. However, an unsymmetric alternative substrate, 3,4-dihydroxybenzoate (PCA), specifically labeled with ^{17}O in either OH group, causes broadening of the EPR spectra observed from the ternary 2,3-CTD·PCA·NO complex irrespective of the location of the ^{17}O label. This result strongly suggests that the substrate chelates the iron in the ternary nitrosyl complex and that there are three sites in the iron coordination sphere that can be occupied by exogenous ligands.

Very recently, Bertini et al. reported X-ray absorption spectroscopic (XAS) studies of 2,3-CTD from *Pseudomonas putida* mt-2 (Bertini et al., 1994a) and its interactions with substrate and inhibitors (Bertini et al., 1994b). A six-coordinate geometry is proposed for the Fe(II) center in the uncomplexed enzyme as well as its complexes with substrate and inhibitors. This conclusion is not substantiated in the present XAS study of the iron site in 2,3-CTD as isolated and the anaerobic substrate complex. Our analysis uses data from both pre-edge and EXAFS regions of the X-ray absorption spectrum together with comparisons of suitable model complexes to show that both 2,3-CTD and its substrate complex are five-coordinate, as originally proposed on the basis of the MCD studies (Mabrouk et al., 1991); these conclusions are consistent with values derived from bond valence sum (BVS) analysis (Brown & Altermatt, 1985; Thorp, 1992). Moreover, our results indicate a fundamental difference in the coordination mode of substrate to Fe(II) and Fe(III) dioxygenases that may be related to their ability to select the site of ring cleavage. The XAS spectrum of the 2,3-CTD·catechol·NO complex has also been investigated. The coordination number of this complex increases to six, perhaps providing the first insight into the structure of the enzyme·substrate·O_2 complex that is the key to Fe(II) dioxygenase chemistry.

EXPERIMENTAL PROCEDURES

Preparation of Samples. Catechol 2,3-dioxygenase was purified from *Pseudomonas putida* mt-2 (ATCC 23973) maintained on *m*-toluic acid and grown on benzoate as the sole carbon source (Arciero et al., 1985). The specific activity of 2,3-CTD was ≥300 units/mg. XAS samples were prepared in either 50 mM potassium phosphate, HEPES, or MOPS at pH 7.5 with 50% glycerol to form glasses when frozen, with final Fe(II) concentrations between 5 and 8 mM. The enzyme·substrate complex was prepared by the anaerobic addition of catechol to a final concentration of 90 mM. The ternary enzyme·substrate·NO complex was made by bubbling NO through an anaerobic enzyme·substrate solution. Anaerobic samples were prepared by repeated evacuation and purging with argon. Samples were frozen with liquid N_2 and stored at 77 K.

The synthesis and characterization of the model complex $[Fe^{II}(6TLA)(DBCH)](ClO_4)$ are described elsewhere (Chiou, 1994).

X-ray Absorption Spectroscopic Data Collection and Analysis. X-ray absorption spectra were collected between 6.95 and 8.0 keV at beam line X9 of the National Synchrotron Light Source (NSLS) at Brookhaven National Laboratory. The monochromator was calibrated using the pre-edge peak at 7113.0 eV in the XAS spectrum of $[Et_4N][FeCl_4]$ (suspended in Duco cement). The XAS data for the model complexes were obtained in transmission mode ($A_{exp} = -\log I_t/I_0$) as 1:1 dispersions of the microcrystalline solid in boron nitride at room temperature. The XAS data for the protein samples were obtained as frozen solutions at 77 K in fluorescence mode. The XAS A_{exp} (C_f/C_0) was determined from the counts observed from the incident (C_0) and fluorescence (C_f) detectors. A 13-element Ge solid state detector (Canberra) was used with a Mn filter and Soller slits (Stern & Heald, 1979).

The pre-edge areas were calculated by subtracting an arctangent function from the data and normalizing with respect to the edge jump height. The background function was determined by a least-squares fit of an arctangent together with a first-order polynomial to the data below the inflection point of the edge, as previously described (Roe et al., 1984). The area of the pre-edge peak, after background subtraction, was obtained by integrating over a range of ~8 eV. This range centered on the peak, and any residual background function was interpolated beyond that range. The edge jump was determined by fitting first-order polynomials to the data as shown previously (Roe et al., 1984). The difference between these two lines at the inflection point of the edge was used as the normalization factor for the pre-edge peak area. For example, 2,3-CTD has a normalized pre-edge peak area of 10.1×10^{-2} eV, which is abbreviated as 10.1 units.

The extraction of χ from the raw EXAFS data (A_{exp}), as discussed in detail in several review papers (Teo, 1981; Scott, 1985), was done by using a modification of the program EXAPLT. χ is the fractional difference in the iron K-shell absorption of the sample relative to that of the monoatomic iron gas. Details of our data treatment procedure, including the correction of fluorescence data for thickness effects and detector response, have been presented previously (Scarrow et al., 1987).

On the basis of single-scattering EXAFS theory, which allows each shell to be modeled separately, EXAFS can be described as a sum of each shell:

$$\chi_c = \sum nA[f(k)k^{-1}r^{-2}\exp(-2\sigma^2k^2)\sin[2kr + \alpha(k)]] \quad (1)$$

where the photoelectron wave vector k equals $[8\pi^2m_e(E - E_0 + \Delta E)/h^2]^{1/2}$. Our analysis procedure, a variation of FABM (fine adjustment based on models) (Teo et al., 1983), uses theoretically calculated phase and amplitude functions

based on a curved-wave formalism (McKale et al., 1988). The amplitude reduction factor (A) and the shell-specific edge shift (ΔE) are empirical parameters obtained from crystallographically characterized model complexes (Scarrow et al., 1987). They partially compensate for imperfections in the amplitude and phase functions f and α (Teo & Lee, 1979). This leaves two parameters per shell, r and n (or σ^2), to be refined at one time. Least-squares refinements were employed on $k^3\chi$ data, and the function minimized was $R \equiv \{\sum k^6(\chi_c - \chi)^2/N\}^{1/2}$, where the sum is over N (~300) data points between 2.0 and 13.0 Å^{-1}, which affords a bond length resolution of 0.14 Å. For each shell, the fitting results show the average iron−ligand distances (r), the type and number (n) of the scatterers, and the Debye−Waller factor σ^2 (in units of Å^2) that can be used to evaluate the distribution of Fe−ligand bond lengths in each shell. The overall quality of a fit for the EXAFS data is judged on the basis of (a) the σ^2 values, which should typically range from 0 to 0.005 Å^2 in each shell, and (b) the magnitude of the fitting residual, RMS_{dev}/RMS_{dat}, of the $k^3\chi$ data, which is an evaluation of the difference between the simulated spectrum and the original Fourier-filtered data.

Calculations of the Bond Valence Sum (BVS). The BVS method has been applied to our results to test the validity of the structural models proposed for the 2,3-CTD complexes by the XAS analysis. The bond valence (BV) of a certain metal−ligand bond with length r is calculated according to (Brown & Altermatt, 1985)

$$BV = \exp[(r_o - r)/B] \quad (B = 0.37 \text{ Å}) \qquad (2)$$

where r_o is obtained from a published database (Liu & Thorp, 1993). For example, r_o for Fe^{II}−O bonds is 1.700 Å and for Fe^{II}−N bonds it is 1.769 Å. The BVS for a given metal center is the sum of bond valences for all of the bonds around that metal ion.

RESULTS

Preedge Data

The X-ray absorption spectra of iron complexes contain a small peak about 10 eV below the midpoint of the K absorption edge, which can be assigned to the iron 1s→3d transition (Shulman et al., 1976). A study of iron(III) model compounds, which included molecular orbital calculations (Roe et al., 1984), has shown that the intensity of pre-edge peaks relative to the K-edge absorption intensity can be correlated with the amount of iron 4p and 3d orbital mixing and, therefore, with the coordination geometry around the iron atom. The pre-edge intensity increases with departure from a centrosymmetric coordination environment and a decrease in coordination number, i.e., $I_{octahedral} < I_{5\text{-coord}} < I_{tetrahedral}$. Our interest in Fe(II) enzymes has recently led us to assemble a pre-edge area database of high-spin Fe(II) complexes (Randall et al., 1995) similar to that previously assembled for the Fe(III) complexes (Roe et al., 1984). In general, Fe(II) complexes exhibit smaller peak areas than Fe(III) complexes having the same coordination number, probably due to the smaller number of partially filled d orbitals. Furthermore, the Fe(II) complexes can be divided into three separate groups of peak areas: six-coordinate complexes have peak areas that range from 4 to 6 units, five-coordinate complexes have peak areas from 8 to 13 units, and tetrahedral complexes have peak areas around 18 units (Randall et al., 1995).

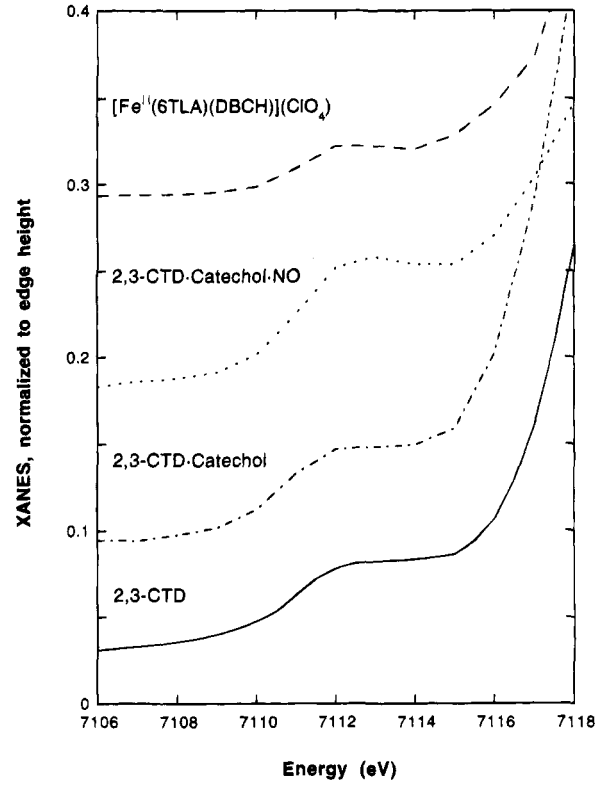

FIGURE 1: Fe K-edge pre-edge features of 2,3-CTD samples.

The 1s→3d pre-edge features of the 2,3-CTD complexes are shown in Figure 1. The peak intensities for 2,3-CTD and the 2,3-CTD·catechol complex are 10.1 and 11.1 units, respectively. Both values fall into the range typical of five-coordinate iron(II) complexes, indicating that 2,3-CTD and its substrate complex have active sites with five-coordinate Fe(II) centers. The 2,3-CTD·catechol·NO ternary complex has a pre-edge area of 14.8 units, which is comparable to those of the six-coordinate Fe^{II}−nitrosyl model complexes (Randall et al., 1995) and the Fe(II) isopenicillin N synthase (IPNS)·ACV·NO complex (Randall et al., 1993). In these complexes, the short Fe−$N_{nitrosyl}$ bond (~1.75 Å) produces substantial distortion from octahedral symmetry and consequently enhances 3d−4p mixing, which results in the unusually large pre-edge areas typically observed. A similar increase in pre-edge signal intensity has been observed among (μ-oxo)diiron(III) complexes due to the distortion derived from the presence of a short Fe−oxo bond (1.74−1.80 Å) (Roe et al., 1984).

The pre-edge area of the enzyme·substrate model complex [Fe^{II}(6TLA)(DBCH)](ClO$_4$) is integrated to be 5.9 units, which is higher than the values for most six-coordinate Fe(II) complexes (Randall et al., 1995). It implies a distorted six-coordinate geometry for this Fe(II) center, a conclusion consistent with the crystal structure of the complex (Chiou, 1994).

EXAFS Studies

2,3-CTD As Isolated. Figure 2 shows the raw EXAFS data obtained for 2,3-CTD, its substrate complex, and the 2,3-CTD·catechol·NO ternary complex. After Fourier filtering, fits to the first-sphere EXAFS data of 2,3-CTD were attempted with different coordination numbers. The best fit is obtained by modeling the first coordination sphere with one shell of five nitrogen and/or oxygen scatterers at 2.09

Table 1: Restricted Fits to the Fourier-Filtered First-Sphere $k^3\chi$ Data of 2,3-CTD Species and the ES Model Complex $[Fe^{II}(TLA)(DBCH)](ClO_4)$

fit	n	Fe−O/N (Å)	σ^2 (Å^2)	n	Fe−O/N (Å)	σ^2 (Å^2)	n	Fe−O/N (Å)	σ^2 (Å^2)	RMS_{dev}/RMS_{dat} (%)
					Native 2,3-CTD[a]					
1	6	2.09	0.0060							15.5
2	4	2.09	0.0026							12.4
3	5	2.09	0.0043							7.1
4	4	2.07	0.0020	1	2.21	−0.0013				6.0
5	3	2.06	0.0005	2	2.19	−0.0005				5.2
6	4	2.09	0.0030	1(S)	2.33	0.0156				8.8
7	5	2.09	0.0043	1(O)	2.45	0.0169				5.1
8	5	2.09	0.0043	1(C)	2.52	0.0075				4.8
					2,3-CTD + Catechol[a]					
9	6	2.08	0.0081							23.5
10	4	2.08	0.0038							18.6
11	5	2.08	0.0059							17.9
12	4	2.10	0.0026	1	1.93	0.0038				6.2
13	3	2.11	0.0018	2	1.99	0.0086				6.3
					$[Fe^{II}(TLA)(DBCH)](ClO_4)$[b]					
14	6	2.24	0.0172							61.7
15	5	2.25	0.0077	1	1.94	0.0009				8.8
16	4	2.26	0.0037	2	1.96	0.0091				18.4
17	5	2.26	0.0058	2	1.95	0.0068				15.1
					2,3-CTD + Catechol + NO[a]					
18	6	2.07	0.0133							45.0
19	5	2.07	0.0089				1	1.78	0.0075	18.8
20	4	2.09	0.0047	1	1.93	0.0027	1	1.74	0.0057	11.1
21	3	2.11	0.0033	2	1.97	0.0060	1	1.74	0.0059	10.5

[a] Refinement and Fourier transform range, 2.0−13.0 Å^{-1}; back-transform range, 0.9−2.2 Å. [b] Refinement and Fourier transform range, 2.0−14.0 Å^{-1}; back-transform range, 1.1−2.1 Å.

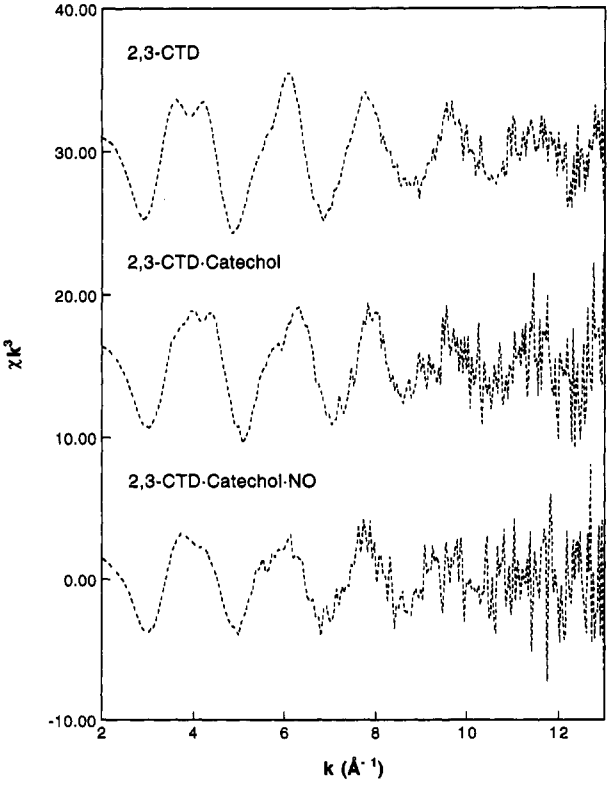

FIGURE 2: Fe K-edge EXAFS spectra of 2,3-CTD samples.

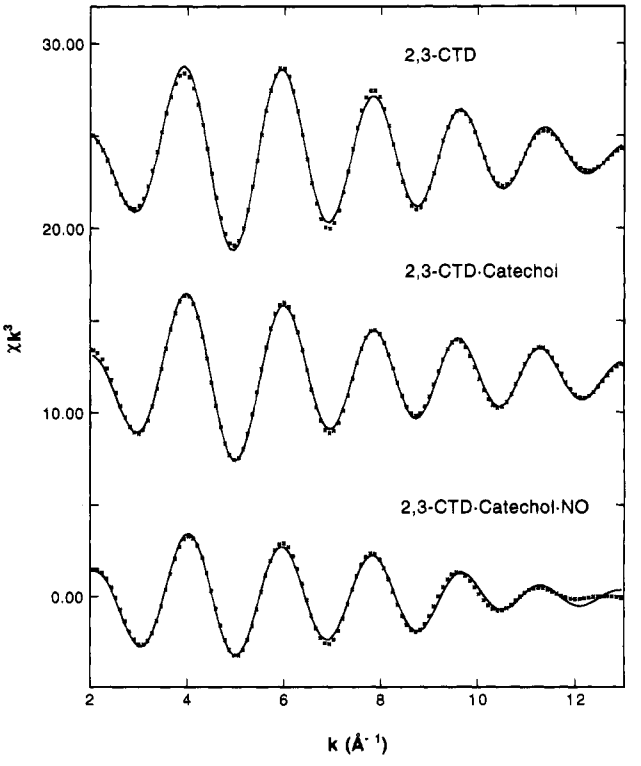

FIGURE 3: Fourier-filtered k^3-weighted EXAFS data (×) and first coordination sphere fits (—) using parameters from fit 3 (Table 1) of 2,3-CTD, fit 12 of 2,3-CTD·catechol, and fit 20 of 2,3-CTD·catechol·NO. The back-transform range was 0.9−2.2 Å.

Å (fit 3, Table 1). It reproduces the Fourier-filtered EXAFS data well and also its Fourier transform (Figures 3 and 4), as indicated by its comparatively low residual (RMS_{dev}/RMS_{dat}) of 7.1%. In contrast, the fits with coordination numbers of six and four have substantially higher residuals (15.5% and 12.4%, fits 1 and 2, respectively, Table 1). Slight improvements to the fit of the data can be obtained by dividing the first coordination sphere into two shells of scatterers. For example, four N/O scatterers at 2.07 Å and one at 2.21 Å or three at 2.06 Å and two at 2.19 Å (fits 4 and 5, Table 1) give improved fits. However, the small

changes in the residual do not justify the inclusion of a second shell. Furthermore, the new shells require negative Debye−Waller factors (σ^2), which are unreasonable.

Two other variations were explored but discarded as unreasonable. Fit 6 involves the addition of a sulfur scatterer, but it has an extremely large σ^2 value of 0.0156.[3] Fits 7 and 8 involve the addition of a low Z scatterer at ca. 2.5 Å, which might arise from either the carbon atom of a chelated carboxylate or the more weakly coordinated oxygen of an asymmetrically chelated carboxylate (Randall et al., 1993; True et al., 1990). Fit 7 is not a good fit because the Fe−O shell at 2.45 Å has an unreasonably large σ^2 value. The Fe−C shell in fit 8, on the other hand, has a marginally acceptable Debye−Waller factor, but decreases the residual by only 30% relative to fit 3 without the carbon scatterer. In the fits for Fe^{II}IPNS (Randall et al., 1993) and the complex of protocatechuate 3,4-dioxygenase (3,4-PCD) with terephthalate (True et al., 1990), the inclusion of a scatterer ca. 2.5 Å to the EXAFS fits significantly improved the residual and modeled features in the EXAFS data not accounted for without the inclusion of the 2.5 Å scatterer. Since this is not the case for 2,3-CTD, our EXAFS analysis indicates that a carboxylate ligand, if present in the active site of 2,3-CTD, is unlikely to be coordinated in a bidentate fashion.

2,3-CTD·Catechol Complex and a Synthetic Analog. Although the Fourier-filtered EXAFS spectra of 2,3-CTD and its catechol complex are rather similar (Figure 3), there is a more pronounced shoulder at $r' = 1.4$ Å in the Fourier-transformed EXAFS spectrum of the 2,3-CTD·catechol complex (Figure 4). In fact, the first coordination sphere of the 2,3-CTD·catechol complex cannot be modeled adequately with a single shell of nitrogen/oxygen scatterers (fits 9−11 in Table 1). In contrast to the analysis for uncomplexed 2,3-CTD, splitting of the first coordination shell significantly improves the fit. The residual is decreased by a factor of almost 3 for fits 12 and 13 relative to fit 11 (Table 1), due to the better fit to the shoulder in the Fourier-transformed spectrum. Fit 12 has one N/O at 1.93 Å and four N/O's at 2.10 Å; while in fit 13 there are two N/O's at 1.99 Å and three N/O's at 2.11 Å. The large σ^2 value of 0.0086 for the 1.99 Å shell in fit 13 is indicative of a large range of metal−ligand distances for the two scatterers composing the shell, which probably results from the combination of one scatterer at 2.10 Å and the other at 1.93 Å resolved from fit 12. Fit 12 thus represents a better model for describing the coordination geometry of the iron center in the 2,3-CTD·catechol complex; substrate binding apparently engenders one short Fe−N/O interaction not present in 2,3-CTD as isolated.

The interpretation of the EXAFS data for the anaerobic 2,3-CTD·catechol complex is greatly facilitated by the EXAFS analysis of $[Fe^{II}(6TLA)(DBCH)](ClO_4)$, the first crystallographically characterized mononuclear Fe(II)−catechol complex (Chiou, 1994). A representation of the structure derived from X-ray crystallography is shown in Figure 5, revealing a catecholate ligand asymmetrically chelated to the iron center with Fe−O bond lengths of 1.953(8) and 2.263(8) Å. On the basis of charge balance, elemental analysis, and spectroscopic features, the coordinated catechol is a monoanionic species in which the protonated oxygen has the longer Fe−O distance (Chiou, 1994).

The analysis of the X-ray absorption spectroscopic data obtained for $[Fe^{II}(6TLA)(DBCH)](ClO_4)$ is in agreement with the crystal structure data. The first-shell contribution to the EXAFS of $[Fe^{II}(6TLA)(DBCH)](ClO_4)$ is poorly modeled by one shell of six scatterers (fit 14 in Table 1). In contrast,

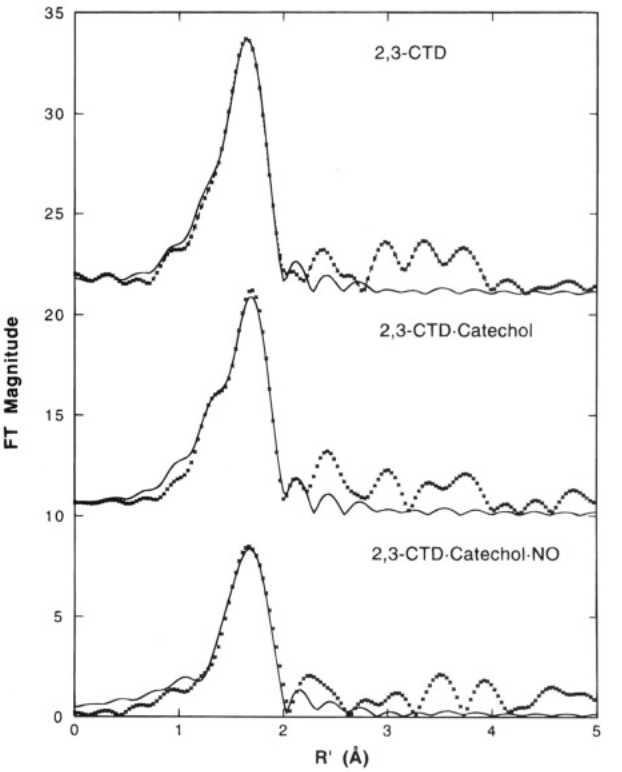

FIGURE 4: Fourier transforms of EXAFS data (×) and first coordination sphere fits (−) of 2,3-CTD (fit 3), 2,3-CTD·catechol (fit 12), and 2,3-CTD·catechol·NO (fit 20). The transform range was 2.0−13.0 $Å^{-1}$.

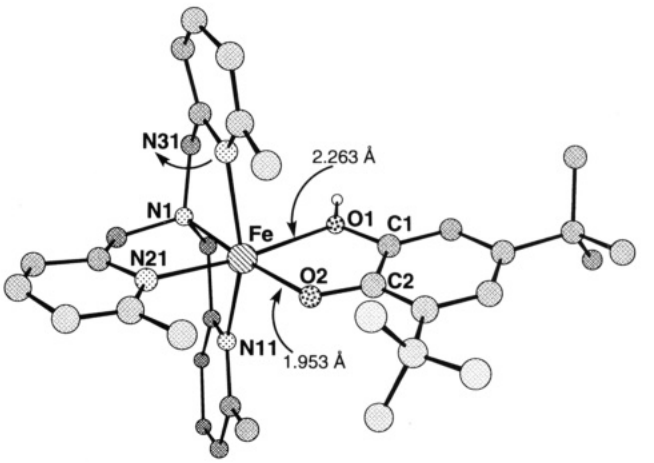

FIGURE 5: Chem 3D representation of the crystal structure of $[Fe^{II}(6TLA)(DBCH)](ClO_4)$. Selected bond lengths (angstroms) and angles (degrees) are as follows: Fe−O1, 2.263(8); Fe−O2, 1.953(8); Fe−N1, 2.21(1); Fe−N11, 2.30(1); Fe−N21, 2.172(9); Fe−N31, 2.31(1); O1−C1, 1.40(1); O2−C2, 1.35(1); C1−C2, 1.40(2); O1−Fe−O2, 76.8(3); O1−Fe−N1, 90.9(3); O2−Fe−N21, 110.9(3); N1−Fe−N21, 81.7(3).

[3] This value is comparable to the one obtained in the fit of EXAFS data for Fe^{II}IPNS (Scott et al., 1992), which in fact has no sulfur ligated to the iron center, as evidenced by other spectroscopic studies (Ming et al., 1990; Ming & Que, 1991; Jiang et al., 1991; Orville et al., 1992). On the other hand, when sulfur is present as one of the ligand atoms of the iron center, as in the Fe^{II}IPNS·ACV complex and $[(TPA)Fe(SC_6H_2\text{-}2,4,6\text{-}Me_3)](ClO_4)$ (Randall et al., 1993), the σ^2 value for the Fe−S shell is on the order of 10^{-3}, which is similar to those of the shells composed of other atoms.

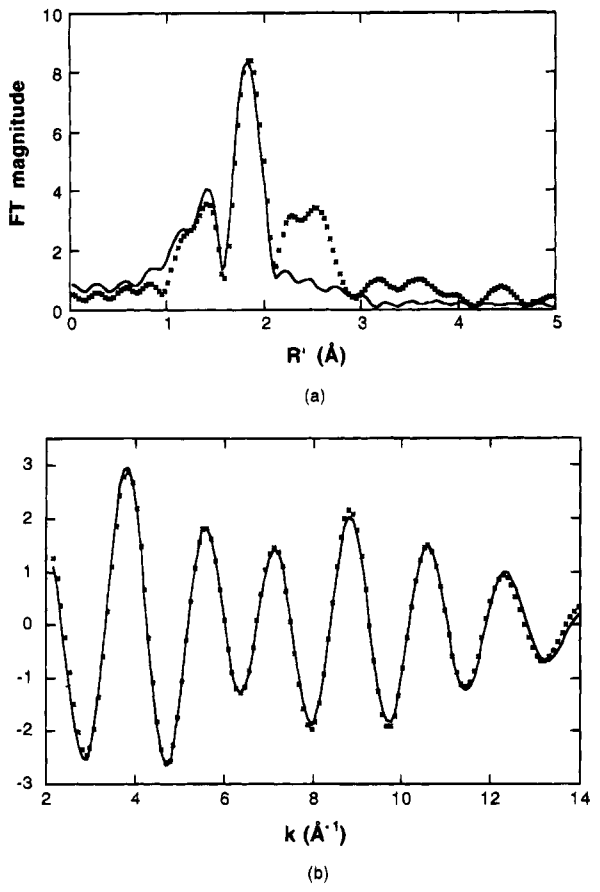

FIGURE 6: Fourier transform (a) and Fourier-filtered k^3-weighted (b) EXAFS spectra of [Fe^{II}(6TLA)(DBCH)](ClO_4): (×) experimental data; (—) first coordination sphere fit using parameters from fit 15. The transform and back-transform ranges were 2.0−14.0 $Å^{-1}$ and 1.1−2.1 Å, respectively.

fit 15, having one N/O scatterer at 1.94 Å and five N/O scatterers at 2.25 Å, has reasonable σ^2 values and a low residual (RMS_{dev}/RMS_{dat}). Furthermore, this fit is in very close agreement to the bond distances obtained from the X-ray crystal structure (one short Fe−ligand bond of 1.95 Å and five other bonds with an average length of 2.25 Å). Among all of the fits tried with different coordination numbers or split shells (see fits 14−17), fit 15 thus is considered to be the best model of the first coordination sphere of [Fe^{II}(6TLA)(DBCH)](ClO_4) (Figure 6). The novel feature of this structure is the coordination of 3,5-di-*tert*-butylcatechol as a monoanion in the complex, giving rise to one short Fe^{II}−O bond. Accordingly, the one short Fe−N/O bond in the 2,3-CTD·catechol complex may arise from a similar coordination mode.

2,3-CTD·Catechol·NO Complex. The Fe K-edge absorption energy is observed to shift from 7121.5 to 7123.5 eV when NO is added to the 2,3-CTD ES complex; this upshift is in agreement with those observed for FeEDTA−NO and Fe^{II}IPNS·ACV·NO relative to their Fe(II) precursors (Brown et al., 1995; Randall et al., 1993).

Fits to the EXAFS data of the 2,3-CTD·catechol·NO complex require three shells for the first coordination sphere of the Fe(II) site. Fit 18 (Table 1) shows that the first sphere cannot be modeled adequately with one shell of six N/O scatterers. The extremely large σ^2 value for this shell strongly suggests a wide distribution of distances for these ligand atoms. The inclusion of a scatterer at ca. 1.78 Å (fit 19) is essential to reproduce the EXAFS spectrum. In other Fe(II)−nitrosyl complexes, such a short distance scatterer arises from the nitrogen atom of the bound nitric oxide (Randall et al., 1993; Westre et al., 1994). Further splitting of the five-scatterer shell in fit 19 is required to lower its apparently high σ^2 value (0.0089) and obtain a smaller fit residual; fits 20 and 21 both reproduce the EXAFS spectra indistinguishably well (Figures 3 and 4). In both fits, the σ^2 value of the NO scatterer is somewhat larger than those associated with the NO scatterers in Fe^{II}IPNS·ACV·NO and [Fe^{II}(TMPzA)Cl(NO)](BPh_4) (Randall et al., 1993). To test the possibility that the NO site may be only partially occupied in 2,3-CTD·catechol·NO, fits varying the NO occupancy from 0.5 to 1 were carried out; in no case did the fit residual improve. Thus, the large σ^2 value is not understood. It is noted, however, that [Fe(TMC)NO](BF_4)$_2$ and [Fe(salen)-NO] both have large σ^2 values associated with their NO scatterers (Westre et al., 1994). Besides the scatterer from nitric oxide, fit 20 has one N/O scatterer at ca. 1.93 Å and four at ca. 2.09 Å, a bond length distribution nearly identical to that found in the enzyme·substrate complex. On the other hand, fit 21 has two scatterers at 1.97 Å and three at 2.11 Å.

Attempts were also made to model the outer coordination spheres in all three 2,3-CTD species. However, because the addition of the back-scattering contributions from the outer spheres did not show a significant effect on the parameters of the first coordination sphere, they are not included in the present discussion.

BVS Calculations

Bond valence sum (BVS) analysis can serve as a check of the chemical fidelity of a given EXAFS model. The basis for the BVS analysis comes from the simple chemical principle that, in a metal complex, there is a compromise between the strength of the metal−ligand bonds and the total number of bonds to keep the metal ion at a certain oxidation state. The strength of a metal−ligand bond can be evaluated from the relative length of that bond, which is termed ($r_o - r$) (cf. eq 2). On the basis of the examination of a large number of crystallographically characterized model complexes, it has been proposed that the BVS value of a metal ion in a complex should be close to the oxidation number of the atom (Brown & Altermatt, 1985; Thorp, 1992). The difference between the BVS value and the oxidation state obtained from other spectroscopic measurements is less than ±0.25 unit. Therefore, BVS analysis is useful in determining the agreement between a given oxidation state for a metal ion and a particular coordination model, which is usually based on EXAFS analysis in the case of metalloproteins. This technique has already been used successfully to test the probable coordination numbers or determine the metal ion oxidation states in a variety of metalloproteins (Liu & Thorp, 1993; Scarrow et al., 1994).

BVS values thus have been calculated for the 2,3-CTD coordination environments determined from the EXAFS fits (Table 2). For the uncomplexed enzyme, the six-coordinate model affords a BVS value of 2.36 units, which is far beyond the range for Fe(II) species (2 ± 0.25). However, a coordination number of five lowers the BVS significantly, so that it is within the proper range. Similarly, for the 2,3-CTD catechol complex, the BVS for fit 12 is almost 2 units,

Table 2: BVS Results for 2,3-CTD Samples

sample	geometry	BVS
2,3-CTD	4O at 2.02 Å, 2N at 2.17 Å[a]	2.36
	5N/O at 2.09 Å[b]	1.91
2,3-CTD•catechol	4O at 1.97 Å, 2N at 2.11 Å[c]	2.72
	4N/O at 2.10 Å, 1N/O at 1.93 Å[b]	2.02
2,3-CTD•catechol•NO	4N/O at 2.09 Å, 1N/O at 1.93 Å, 1N/O at 1.74 Å[b]	3.13
	3N/O at 2.11 Å, 2N/O at 1.97 Å, 1N/O at 1.74 Å[b]	3.21
[(TMPzA)Fe(NO)Cl](BPh$_4$)	1N at 1.74 Å, 3N at 2.16 Å, 1N at 2.29 Å, 1Cl at 2.34 Å[d]	2.96
[(TMPzA)Fe(NO)(ClO$_4$)](BPh$_4$)	1N at 1.77 Å, 3N at 2.1 Å, 1O at 2.23 Å, 1N at 2.28 Å[e]	2.71
[(TPA)Fe(BF)(NO)](ClO$_4$)	1N at 1.72 Å, 1O at 2.05 Å, 4N at 2.16 Å[f]	2.92

[a] Bertini et al., 1994a. [b] This work; r_o (1.7345 Å) is taken as the average of r_o(Fe−O) and r_o(Fe−N), which is reasonable since the crystal structure of the 2,3-dihydroxybiphenyl 1,2-dioxygenase shows an iron site with a 2N/3O coordination environment. [c] Bertini et al., 1994b. [d] Randall et al., 1993. [e] Y. Zang, L.-J. Ming, and L. Que, Jr., personal communication. [f] Chiou, 1994.

which indicates that the coordination number and the bond distances are appropriate. The BVS value for the 2,3-CTD•substrate•NO complex, on the other hand, is calculated to be even larger than 3. As a comparison, the BVS values calculated from the crystal structures of three Fe^{II}−nitrosyl complexes are also around 3 (Table 2). The increased BVS value upon NO binding is consistent with the notion that the coordination of NO results in the transfer of an electron from the iron center, affording an Fe^{III}−NO^- moiety (Zhang et al., 1992; Brown et al., 1995).

DISCUSSION

The XAS results reported here (both pre-edge and EXAFS data) indicate a five-coordinate structure for the Fe(II) active site in 2,3-CTD and its substrate complex. This conclusion is in line with results from previous MCD studies (Mabrouk et al., 1991) indicating that the Fe(II) site possesses square-pyramidal coordination geometry in both species. It is also corroborated by the emerging crystal structure of another extradiol-cleaving enzyme, 2,3-dihydroxybiphenyl 1,2-dioxygenase, which shows a five-coordinate square-pyramidal Fe(II) center ligated to one axial His and four basal ligands (one His, one Glu, and two solvent waters) (J. T. Bolin, S. Han, and L. D. Eltis, personal communication). However, our results differ from those reported recently by Bertini et al. (1994a,b), who favor a six-coordinate iron center for 2,3-CTD in the five complexes studied (*vide infra*).

Our best fit to the data for 2,3-CTD as isolated (fit 3, Table 1) consists of a single shell of five scatterers with an average distance of 2.09 Å. The reasonably low σ^2 value of 0.0043 associated with this shell in the fit implies that the bond distances of these ligands are distributed over a small range; the five ligand atoms likely are similar in charge, size, and atomic number. The bond distances associated with 2,3-CTD are in accord with the 2.06−2.13 Å range found for the Fe(II) bonds with aromatic nitrogen donors in five-coordinate environments (Kitajima et al., 1994; Ménage et al., 1990; Stassinopoulos et al., 1991; Zang & Que, 1995) or the 2.11 Å distance associated with a neutral oxygen ligand such as H_2O (Hamalainen & Turpeinen, 1989). Thus, the bound solvent molecules in 2,3-CTD are more likely to be water rather than hydroxide as postulated for Fe^{II}IPNS, where the Fe−solvent distance was found to be around 2.01 Å (Randall et al., 1993). The crystal structure of 2,3-dihydroxybiphenyl 1,2-dioxygenase shows the presence of a monodentate carboxylate ligand (J. T. Bolin, S. Han, and L. D. Eltis, personal communication). Unlike the cases of Fe^{II}-IPNS and the 3,4-PCD•terephthalate complex, there is no feature in the EXAFS spectrum of 2,3-CTD that unequivocally requires a chelated carboxylate ligand. For example, there is no evidence for a scatterer at ca. 2.5 Å, as may arise from a chelated carboxylate (Randall et al., 1993; True at al., 1990). However, a monodentate carboxylate ligand would be expected to give rise to an Fe−O distance of ca. 2.01−2.14 Å (Tolman et al., 1991; Hagen & Lachicotte, 1992; Chiou & Que, 1995), which can easily be accommodated by the average 2.09 Å distance associated with the first shell. Thus, the EXAFS data for uncomplexed 2,3-CTD are consistent with the crystal structure and follow the His/carboxylate/solvent motif that is emerging among the active sites of mononuclear non-heme Fe(II) enzymes, such as superoxide dismutase (Lah et al., 1995; Stoddard et al., 1990), soybean lipoxygenase (Boyington et al., 1993; Minor et al., 1993), and Fe^{II}IPNS (Randall et al., 1993).

According to our XAS analysis, substrate binding to 2,3-CTD maintains the five-coordinate environment found in the enzyme as isolated, in agreement with the MCD data (Mabrouk et al., 1991). A significant result from this study is the appearance of a new N/O scatterer at 1.93 Å in the ES complex, replacing one of the 2.09 Å scatterers in the unligated enzyme. It is very likely that this new scatterer arises from the coordination of substrate. The interpretation of this new feature has been greatly facilitated by the model complex [Fe^{II}(6TLA)(DBCH)](ClO$_4$) (Chiou, 1994), which has a monoanionic catecholate ligand that is unsymmetrically chelated to the Fe(II) center (r_{Fe-O} = 1.95 and 2.26 Å). In the model, the short bond comes from the negatively charged oxygen of 3,5 di-*t*-butylcatecholate and falls into the range of Fe^{II}−$O_{phenolate}$ bond distances found in other Fe(II) model complexes (Stassinopoulos et al., 1991; Nasri et al., 1987; Jameson et al., 1978; Cini, 1983). The similar lengths of the Fe−$O_{catecholate}$ bond in [Fe^{II}(6TLA)(DBCH)](ClO$_4$) and of the new scatterer in the 2,3-CTD ES complex strongly suggest that the latter derives from the catecholate oxygen of the substrate.

Our EXAFS analysis results do not allow us to determine whether the other catecholate oxygen is bound to the metal center. However, the EPR studies on the E•S•NO complex indicate that both catecholate oxygens are coordinated to the metal center, displacing the solvent molecules found in the isolated enzyme (Arciero & Lipscomb, 1986). Although the coordination of the second catecholate oxygen and the displacement of solvent molecules may occur upon the binding of NO to the ES complex, it seems more reasonable to us that these structural changes occur in the ES complex, so as to poise the iron(II) center for the facile binding of O_2

(or NO). Indeed, it is clear that the affinity of the enzyme for NO dramatically increases in the presence of substrate (Arciero et al., 1985). The other substrate oxygen, if ligated to the Fe(II) center, must have a bond length close to the 2.10 Å found for the remaining four scatterers in the ES complex, which would be significantly shorter than that found for the Fe−O bond to the protonated catechol oxygen in the model complex (2.26 Å). While this shortening may be a result of the deprotonation of the second catecholate oxygen, it is unlikely because of the lower Lewis acidity of Fe(II) and its low affinity for catecholate (Harris et al., 1979). We thus favor a monoanionic bidentate catecholate in the ES complex. Two factors may contribute to the shortening of the second $Fe-O_{catechol}$ bond in the ES complex relative to that found in $[Fe^{II}(6TLA)(DBCH)](ClO_4)$: (a) the five-coordinate geometry, which shortens metal−ligand bond lengths relative to six-coordinate geometries, and (b) the presence of an active site base that can hydrogen bond to the catecholate OH, which would make the oxygen a better ligand to the iron. The latter factor is supported by the crystal structure of 2,3-dihydroxybiphenyl 1,2-dioxygenase (J. T. Bolin, S. Han, and L. D. Eltis, personal communication), which shows two nonligating histidine residues in the vicinity of the iron(II) active site.

Our XAS results indicate that the iron center becomes six-coordinate in the E·S·NO complex, suggesting that the metal coordination sphere expands upon NO (and presumably O_2) binding. Accordingly, NO likely binds at the vacant sixth site in the ES complex. It is interesting to note that the presence of NO does not seem to significantly affect the average iron−ligand bond lengths derived from the endogenous ligands and bound substrate (Δr = 0.01 Å from the ES complex to the E·S·NO complex). The small change observed in this case is comparable to that found for the $[Fe^{II}(TPA)BF(MeOH)]^+/[Fe(TPA)BF(NO)]^+$ pair, both of which are characterized crystallographically (Chiou, 1994; Chiou & Que, 1995), but contrasts with the significant shortening (>0.1 Å) observed in EXAFS studies of the $[Fe(OH_2)(EDTA)]^{2-}$/FeEDTA-NO pair (Westre et al., 1994). Two factors play a role in determining the iron−ligand lengths upon the addition of NO to the 2,3-CTD ES complex and exert opposing effects: (a) the expansion of the iron coordination sphere by 1, which is expected to lengthen the iron−ligand bonds, and (b) the decrease in the ionic radius of the iron center due to its partial oxidation upon NO addition, as indicated by the Fe K-edge shift and the BVS calculations. The partial oxidation of the iron center upon NO binding is implied by the $Fe^{III}-NO^-$ description favored for the $\{FeNO\}^7$ system (Zhang et al., 1992; Brown et al., 1995). The combination of these opposing effects affords essentially unperturbed metal−ligand bonds. Because fits 20 and 21 represent comparably reasonable models for the data, the ionization state of the coordinated substrate cannot be established. The substrate may lose its second proton upon NO binding, due to the increased Lewis acidity of the iron center when it is partially oxidized.

Our present XAS results differ from those of Bertini et al. (1994a,b), who favor a six-coordinate iron(II) center for 2,3-CTD in the five complexes that they investigated. We have compared their fits of the enzyme as isolated and the ES complex to those reported here by subjecting them to BVS analysis (Table 2). The BVS values calculated from the six-coordinate sites favored by Bertini et al. are consistently higher than that expected for a high-spin Fe(II) center (2 ± 0.25). In other words, the bond lengths obtained by Bertini et al. are too short for a six-coordinate high-spin Fe(II) center. Our fits, which favor a five-coordinate site, on the other hand, afford BVS values close to the mean value expected for a high-spin Fe(II) center and are in agreement with the recent crystal structure of 2,3-dihydroxybiphenyl 1,2-dioxygenase (J. T. Bolin, S. Han, and L. D. Eltis, personal communication). Although we cannot rationalize why the pre-edge data from the two groups differ, a probable source of the discrepancy between the metal−ligand bond lengths obtained from the two studies is the mode of EXAFS analysis. Bertini et al. used the program EXCURV88, which appears to underestimate the metal−ligand bond distances in iron complexes (Scarrow et al., 1994). Indeed, when EXAFS data for the model complex $[Fe(N\text{-Me-im})_6](BPh_4)_2$ were fit by using the EXCURVE88 protocol as a test case, the Fe−N distances were underestimated by as much as 0.05 Å, a substantial discrepancy (Scarrow et al., 1994). Similarly, Scarrow et al. also found disagreements between their interpretation of the EXAFS data for soybean lipoxygenase and those previously published by groups using the EXCURVE88 protocol (Navaratnam et al., 1988; Feiters et al., 1990; Van der Heijdt et al., 1992). Again, the latter groups underestimated metal−ligand bond distances, as evidenced by BVS values that were incommensurate with the expected oxidation states of the metal centers. We thus believe that the fits presented here provide a more accurate model of the 2,3-CTD active site, one that is entirely consistent with the picture emerging from X-ray crystallography.

Mechanistic Implications. The reaction mechanism for the Fe(II)-containing extradiol-cleaving catechol dioxygenases such as 2,3-CTD is not as well-understood as that for the Fe(III)-containing intradiol-cleaving enzymes such as 3,4-PCD and catechol 1,2-dioxygenase (1,2-CTD) (Lipscomb & Orville, 1992; Que, 1989). In both classes of dioxygenases, there is no evidence for formal redox cycling during catalysis. For the intradiol-cleaving enzymes, the iron is maintained in the Fe(III) state by the presence of two tyrosinate ligands, which confer a low redox potential to the metal center and give rise to the characteristic red color of these enzymes (Ohlendorf et al., 1988; Pyrz et al., 1985; Que & Epstein, 1981). On the basis of a number of spectroscopic observations (Orville & Lipscomb, 1989; True et al., 1990; Lauffer & Que, 1982; Felton et al., 1978), the substrate is thought to initially chelate as a dianion to the Fe(III) in the active site of 3,4-PCD. Preliminary crystallographic studies of inhibitor complexes suggest that the solvent hydroxide and one endogenous tyrosinate ligand serve as proton acceptors for the two substrate protons and are displaced as the substrate binds (Orville et al., 1993; Ohlendorf et al., 1994). This result stands in marked contrast to the current results, which show that the substrate catechol is very likely to be bound as a monoanion to the Fe(II) center in 2,3-CTD. This difference in catechol binding to the active site iron atoms of the two related classes of dioxygenases may play a role in directing the position of ring opening.

A mechanism for Fe(II) dioxygenases based on our past and current studies is diagrammed in Figure 7. In this scheme, catechol is proposed to chelate the Fe(II) center by replacing two existing ligands. However, because of the weaker Lewis acidity of the Fe(II) center, only one proton is lost upon binding of the substrate. Binding of the substrate

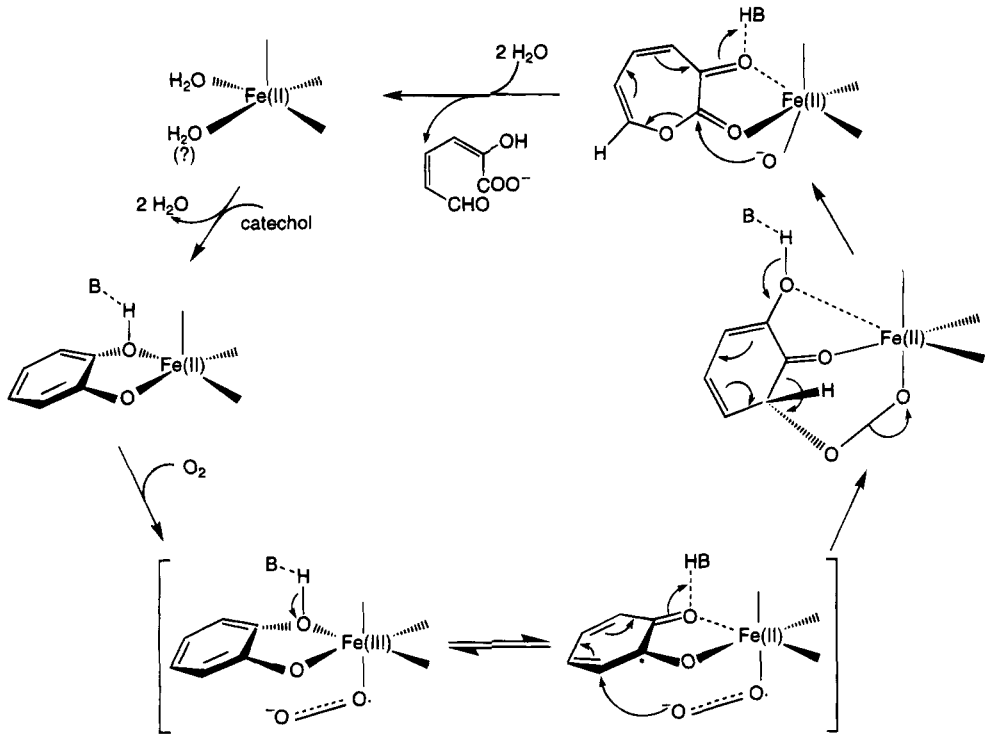

FIGURE 7: Proposed mechanism for extradiol ring cleavage of catechol by 2,3-CTD.

anion to the Fe(II) activates it to bind O_2 at the vacant sixth coordination site. As noted earlier, this is consistent with the 1000-fold increase in NO affinity for the Fe(II) when substrate is bound (Arciero et al., 1985). O_2 binding results in the transfer of charge from Fe(II) to O_2, forming what can be viewed as an Fe(III)−superoxide species. A subsequent shift of electron density from the coordinated catechol to the iron center enhances the nucleophilic attack of the nascent superoxide on the catechol ring to form an intermediate alkylperoxo moiety (Lipscomb & Orville, 1992). Cleavage of the O−O bond, coupled with a ring insertion reaction equivalent to Criegee rearrangement chemistry (Criegee, 1948; Harpel & Lipscomb, 1990), forms a seven-membered lactone ring, which then hydrolyzes to afford the semialdehyde product.

Within the framework of this proposed mechanism, the central questions are as follows: (a) What prevents the direct attack of oxygen on the aromatic ring as proposed for the Fe(III) dioxygenases? (b) What determines the position of attack of the Fe(II)-bound oxygen on the aromatic ring? Although the answers to both of these questions may involve structural constraints within the enzyme active site to some extent, the presence of the Fe(II) center and the asymmetric binding of the catechol indicated by the present study may also play critical roles, as illustrated in Figure 7. For 3,4-PCD, the key to the direct electrophilic attack of the substrate by O_2 is the Fe(III)−dianionic catecholate interaction (Cox & Que, 1988; Jang et al., 1991), which gives rise to a low-energy catecholate-to-Fe(III) charge transfer transition and facilitates O_2 attack on the bound substrate. This attack is also promoted by the tendency of the dianionic catecholate to ketonize as indicated by the strong affinity of the 3,4-PCD active site for α-hydroxypyridine *N*-oxides, which are substrate analogs, that favor a ketonized α-hydroxy group (Lipscomb et al., 1982; May et al., 1982, 1983; Whittaker & Lipscomb, 1984). O_2 binding to the iron center is disfavored because of its Fe(III) oxidation state. For 2,3-CTD, on the other hand, there is no low-energy charge transfer transition: the substrate is bound as a monoanion, and the iron center is in the Fe(II) oxidation state. Direct O_2 attack on the coordinated substrate is disfavored because its monoanionic nature makes it less electron-rich than the dianionic catecholate in 3,4-PCD. Furthermore, the coordination of the substrate to the Fe(II) center lowers its redox potential and activates the metal center for O_2 binding. This line of reasoning rationalizes the initial attack of O_2 on the Fe(II) center.

In our model, the distinction between the modes of ring cleavage depends on the site of dioxygen attack on the aromatic ring. Attack on an oxygen-bearing carbon affords intradiol cleavage, while attack on the carbon adjacent to the oxygen-bearing carbon gives rise to extradiol cleavage. We propose that this distinction rests on whether the dioxygen-attacking moiety is electrophilic or nucleophilic. For the intradiol-cleaving enzymes, the electrophilic O_2 directly attacks an oxygen-bearing carbon atom of the dianionic catecholate, which is made electron-rich by ketonization of the other oxygen-bearing carbon atom. For the extradiol-cleaving enzymes, O_2 binds to the iron(II) center and is converted to a nucleophilic superoxide moiety. Attack on the ring would then occur at sites of low electron density. In Figure 7 (bottom right structure), we show the attack of the superoxide as a 1,6-Michael addition to the ketonized substrate. The combination of these effects, together with the geometric constraints of oxygen and substrate both bound to the iron, would make the carbon ortho to the more strongly bound $Fe-O_{catecholate}$ and meta to the more weakly bound $Fe-O_{catecholate}$ the favored position for nucleophilic attack. Subsequent cleavage of the O−O bond occurs concomitant with extradiol ring cleavage.

CONCLUSIONS

The iron sites of Fe(II) and Fe(III) dioxygenases both appear to be five-coordinate, but the nature of the ligands

present in each case stabilizes different redox states and causes the oxygen activation and insertion chemistries to differ markedly. The work presented here suggests that the redox state of the iron strongly influences the binding mode of the catechol substrate and the subsequent position of O_2 attack. Catecholic substrates appear to bind to the iron center in both classes of dioxygenases, but the loss of only one of the catecholate protons in the case of the Fe(II) enzymes leads to highly asymmetric binding. This, in turn, leads to charge distribution on the ring, which, combined with the nature of the metal-bound dioxygen, directs oxygen attack to a position where extradiol cleavage must occur. In contrast, the ability of the iron in Fe(III) dioxygenases to act as a Lewis acid and the chelation of the catecholic substrate as a dianion lead to direct O_2 attack on the substrate at an oxygen-bearing carbon and ketonization of the hydroxyl function on the adjacent carbon. Subsequent oxygen insertion occurs between the carbon attacked and the carbon carrying the ketonized oxygen, leading to intradiol cleavage.

The XAS studies presented here, considered together with our previous studies of Fe(III) dioxygenases, have allowed us to recognize the unique substrate binding modes of the two major aromatic dioxygenase classes. Moreover, these observations have permitted the development of a mechanistic proposal that provides a rational basis for the remarkable fidelity of ring cleavage position exhibited by each aromatic dioxygenase class.

ACKNOWLEDGMENT

We thank Drs. Anne E. True and Clayton R. Randall for assistance with data collection and initial analysis. We thank Drs. Syed Khalid and Yang Hai at beam line X9 of the NSLS for technical guidance.

REFERENCES

Arciero, D. M., & Lipscomb, J. D. (1986) *J. Biol. Chem. 261*, 2170−2178.
Arciero, D. M., Orville, A. M., & Lipscomb, J. D. (1985) *J. Biol. Chem. 260*, 14035−14044.
Bertini, I., Briganti, F., Mangani, S., Nolting, H. F., & Scozzafava, A. (1994a) *Biochemistry 33*, 10777−10784.
Bertini, I., Briganti, F., Mangani, S., Nolting, H. F., & Scozzafava, A. (1994b) *FEBS Lett. 350*, 207−212.
Boyington, J. C., Gaffney, B. J., & Amzel, L. M. (1993) *Science 260*, 1482−1486.
Brown, I. D., & Altermatt, D. (1985) *Acta Crystallogr. B41*, 244−247.
Brown, C. A., Pavlosky, M. A., Westre, T. E., Zhang, Y., Hedman, B., Hodgson, K. O., & Solomn, E. I. (1995) *J. Am. Chem. Soc. 117*, 715−732.
Chen, V. J., Orville, A. M., Harpel, M. R., Frolik, C. A., Surerus, K. K., Münck, E., & Lipscomb, J. D. (1989) *J. Biol. Chem. 264*, 21677−21681.
Chiou, Y.-M. (1994) Ph.D. Thesis, University of Minnesota, Minneapolis, MN.
Chiou, Y.-M., & Que, L., Jr. (1995) *J. Am. Chem. Soc. 117*, 3999−4013.
Cini, R. (1983) *Inorg. Chim. Acta 73*, 147−152.
Cox, D. D., & Que, L., Jr. (1988) *J. Am. Chem. Soc. 110*, 8085−8092.
Criegee, R. (1948) *Ann. Chem. 560*, 127−135.
Feiters, M. C., Boelens, H., Veldink, G. A., Vliegenthart, J. F. G., Navaratnam, S., Allen, J. C., Nolting, H.-F., & Hermers, C. (1990) *Recl. Trav. Chim. Pays-Bas 109*, 133−146.
Felton, R. H., Cheung, L. D., Philips, R. S., & May, S. W. (1978) *Biochem. Biophys. Res. Commun. 85*, 844−850.
Hagen, K. S., & Lachicotte, R. (1992) *J. Am. Chem. Soc. 114*, 8741−8742.
Hamalainen, R., & Turpeinen, U. (1989) *Acta Chem. Scand. 43*, 15−18.
Harpel, M. R., & Lipscomb, J. D. (1990) *J. Biol. Chem. 265*, 22187−22196.
Harris, W. R., Carrano, C. J., Cooper, S. R., Sofen, S. R., Avdeef, A. E., McArdle, J. V., & Raymond, K. N. (1979) *J. Am. Chem. Soc. 101*, 6097−6104.
Hirata, F., Nakazawa, A., Nozaki, M., & Hayaishi, O. (1971) *J. Biol. Chem. 246*, 5882−5887.
Hori, K., Hashimoto, T., & Nozaki, M. (1973) *J. Biochem. 74*, 375−384.
Jameson, G. B., March, F. C., Robinson, W. T., & Koon, S. S. (1978) *J. Chem. Soc., Dalton Trans.* 185−191.
Jang, H. G., Cox, D. D., & Que, L., Jr. (1991) *J. Am. Chem. Soc. 113*, 9200−9204.
Jiang, F., Peisach, J., Ming, L.-J., Que, L., Jr., & Chen, V. J. (1991) *Biochemistry 30*, 11437−11445.
Kitajima, N., Tamura, N., Amagai, H., Fukui, H., Moro-oka, Y., Mizutani, Y., Kitagawa, T., Mathur, R., Heerwegh, K., Reed, C. A., Randall, C. R., Que, L., Jr., & Tatsumi, K. (1994) *J. Am. Chem. Soc. 116*, 9071−9085.
Lah, M. S., Dixon, M. M., Pattridge, K. A., Stallings, W. C., Fee, J. A., & Ludwig, M. L. (1995) *Biochemistry 34*, 1646−1660.
Lauffer, R. B., & Que, L., Jr. (1982) *J. Am. Chem. Soc. 104*, 7324−7325.
Lipscomb, J. D., & Orville, A. M. (1992) *Metal Ions Biol. Syst. 28*, 243−298.
Lipscomb, J. D., Whittaker, J. W., & Arciero, D. M. ((1982) in *Oxygenases and Oxygen Metabolism* (Nozaki, M., Yamamoto, S., Ishimura, Y., Coon, M. J., Ernster, L. & Estabrook, R. W., Eds.) pp 27−38, Academic, New York.
Liu, W., & Thorp, H. H. (1993) *Inorg. Chem. 32*, 4102−4105.
Mabrouk, P. A., Orville, A. M., Lipscomb, J. D., & Solomon, E. I. (1991) *J. Am. Chem. Soc. 113*, 4053−4061.
May, S. W., Oldham, C. D., Mueller, P. W., Padgette, S. R., & Sowell, A. L. (1982) *J. Biol. Chem. 257*, 12746−12751.
May, S. W., Mueller, P. W., Oldham, C. D., Williamson, C. K., & Sowell, A. L. (1983) *Biochemistry 22*, 5331−5340.
McKale, A. G., Veal, B. W., Paulikas, A. P., Chan, S.-K., & Knapp, G. S. (1988) *J. Am. Chem. Soc. 110*, 3763−3768.
Ménage, S., Brennan, B. A., Juarez-Garcia, C., Münck, E., & Que, L., Jr. (1990) *J. Am. Chem. Soc. 112*, 6423−6425.
Ming, L., & Que, L., Jr. (1991) *Biochemistry 30*, 11653−11659.
Ming, L.-J., Que, L., Jr., Kriauciunas, A., Frolik, C. A., & Chen, V. J. (1990) *Inorg. Chem. 29*, 1111−1112.
Minor, W., Steczko, J., Bolin, J. T., Otwinowski, Z., & Axelrod, B. (1993) *Biochemistry 32*, 6320−6323.
Nakai, C., Hori, K., Kagamiyama, H., Nakazawa, T., & Nozaki, M. (1983) *J. Biol. Chem. 258*, 2916−2922.
Nasri, H. J., Weiss, R., Bill, E., & Trautwein, A. (1987) *J. Am. Chem. Soc. 109*, 2549−2550.
Navaratnam, S., Feiters, M. C., Al-Hakim, M., Allen, J. C., Veldink, G. A., & Vliegenthart, J. F. G. (1988) *Biochim. Biophys. Acta 956*, 70−76.
Nelson, M. J. (1988) *J. Am. Chem. Soc. 110*, 2985−2986.
Nozaki, M., Nakazawa, T., Fujisawa, H., Kotani, S., Kojima, Y., & Hayaishi, O. (1968) *Adv. Chem. Ser. 77*, 242−251.
Ohlendorf, D. H., Lipscomb, J. D., & Weber, P. C. (1988) *Nature 336*, 403−405.
Ohlendorf, D. H., Orville, A. M., & Lipscomb, J. D. (1994) *J. Mol. Biol. 244*, 586−608.
Olson, P. E., Qi, B., Que, L., Jr., & Wackett, L. P. (1992) *Appl. Environ. Microbiol. 58*, 2820−2826.
Orville, A. M., & Lipscomb, J. D. (1989) *J. Biol. Chem. 264*, 8791−8801.
Orville, A. M., Chen, V. J., Kriauciunas, A., Harpel, M. R., Fox, B. G., Münck, E., & Lipscomb, J. D. (1992) *Biochemistry 31*, 4602−4612.
Orville, A. E., Lipscomb, J. D., & Ohlendorf, D. H. (1993) *J. Inorg. Biochem. 51*, 295.
Pyrz, J. W., Roe, A. L., Stern, L. J., & Que, L., Jr. (1985) *J. Am. Chem. Soc. 107*, 614−620.
Que, L., Jr. (1989) in *Iron Carriers and Iron Proteins* (Loehr, T. M., Ed.) pp 467−524, VCH, New York.
Que, L., Jr., & Epstein, R. M. (1981) *Biochemistry 20*, 2545−2550.

Que, L., Jr., Widom, J., & Crawford, R. L. (1981) *J. Biol. Chem. 256*, 10941−10944.

Randall, C. R., Zang, Y., True, A. E., Que, L., Jr., Charnock, J. M., Garner, C. D., Fujishima, Y., Schofield, C. J., & Baldwin, J. E. (1993) *Biochemistry 32*, 6664−6673.

Randall, C. R., Shu, L., Chiou, Y.-M., Hagen, K. S., Ito, M., Kitajima, N., Lachicotte, R. J., Zang, Y., & Que, L., Jr. (1995) *Inorg. Chem. 33*, 1036−1039.

Rich, P. R., Salerno, J. C., Leigh, J. S., & Bonner, W. D. (1978) *FEBS Lett. 93*, 323−326.

Roe, A. L., Schneider, D. J., Mayer, R. J., Pyrz, J. W., Widom, J., & Que, L., Jr. (1984) *J. Am. Chem. Soc. 106*, 1676−1681.

Scarrow, R. C., Maroney, M. J., Palmer, S. M., Roe, A. L., Que, L., Jr., Salowe, S. P., & Stubbe, J. (1987) *J. Am. Chem. Soc. 109*, 7857−7864.

Scarrow, R. C., Trimitsis, M. G., Buck, C. P., Grove, G. N., Cowling, R. A., & Nelson, M. J. (1994) *Biochemistry 33*, 15023−15035.

Scott, R. A. (1985) *Methods Enzymol. 11*, 414−459.

Scott, R. A., Wang, S., Eidsness, M. K., Kriauciunas, A., Frolik, C. A., & Chen, V. J. (1992) *Biochemistry 31*, 4596−4601.

Shulman, R. G., Yafet, Y., Eisenberger, P., & Blumberg, W. E. (1976) *Proc. Natl. Acad. Sci. U.S.A. 73*, 1384−1388.

Stassinopoulos, A., Schulte, G., Papaefthymiou, G. C., & Caradonna, J. P. (1991) *J. Am. Chem. Soc. 113*, 8686−8697.

Stern, E. A., & Heald, S. M. (1979) *Rev. Sci. Instrum. 50*, 1579−1582.

Stoddard, B. L., Howell, P. L., Ringe, D., & Petsko, G. A. (1990) *Biochemistry 29*, 8885−8893.

Tatsuno, Y., Saeki, Y., Nozaki, M., Otsuka, S., & Maeda, Y. (1980) *FEBS Lett. 112*, 83−85.

Teo, B.-K. (1981) in *EXAFS Spectroscopy, Techniques and Applications* (Teo, B.-K., & Joy, D. C., Eds.) pp 13−58, Plenum, New York.

Teo, B.-K., & Lee, P. A. (1979) *J. Am. Chem. Soc. 101*, 2815−2832.

Teo, B.-K., Antonio, M. R., & Averill, B. A. (1983) *J. Am. Chem. Soc. 105*, 3751−3762.

Thorp, H. H. (1992) *Inorg. Chem. 31*, 1585−1588.

Tolman, W. B., Liu, S., Bentsen, J. G., & Lippard, S. J. (1991) *J. Am. Chem. Soc. 113*, 152−164.

True, A. E., Orville, A. M., Pearce, L. L., Lipscomb, J. D., & Que, L., Jr. (1990) *Biochemistry 29*, 10847−10854.

Van der Heijdt, L. M., Feiters, M. C., Navaratnam, S., Nolting, H.-F., Hermes, C., Veldink, G. A., & Vliegenthart, J. F. G. (1992) *Eur. J. Biochem. 207*, 793−802.

Westre, T. E., Cicco, A. D., Filipponi, A., Natoli, C. R., Hedman, B., Solomn, E. I., & Hodgson, K. O. (1994) *J. Am. Chem. Soc. 116*, 6757−6768.

Whittaker, J. W., & Lipscomb, J. D. (1984) *J. Biol. Chem. 259*, 4476−4486.

Zang, Y., & Que, L., Jr. (1995) *Inorg. Chem. 34*, 1030−1035.

Zang, Y., Elgren, T. E., Dong, Y., & Que, L., Jr. (1993) *J. Am. Chem. Soc. 115*, 811−813.

Zhang, Y., Pavlosky, M. A., Brown, C. A., Westre, T. E., Hedman, B., Hodgson, K. O., & Solomon, E. I. (1992) *J. Am. Chem. Soc. 114*, 9189−9191.

BI9426221